

# Active Flexure Compensation Software for the Echellette Spectrograph and Imager on Keck II

Robert Kibrick, Joseph Miller, Jerry Nelson, Matthew Radovan, Andrew Sheinis, and Brian Sutin  
UCO/Lick Observatory, University of California, Santa Cruz, California 95064 USA

## ABSTRACT

All Cassegrain spectrographs suffer from gravitationally-induced flexure to some degree. While such flexure can be minimized via careful attention to mechanical design and fabrication, further performance improvements can be achieved if the spectrograph *has been designed to minimize hysteresis and* has active compensation for any residual flexure. The Echellette Spectrograph and Imager (ESI), built at UCO/Lick Observatory for use at Cassegrain focus on Keck II, compensates for such residual flexure via its collimator mirror. The collimator is driven by three actuators that provide control of collimator focus, tip, and tilt. The ESI control software utilizes a mathematical model of gravitationally-induced flexure to periodically compute and apply flexure corrections by commanding the corresponding tip and tilt motions to the collimator. In addition, the ESI control software provides an optional, manual, closed-loop method for adjusting the collimator position to compensate for any non-repeatable errors. Such errors may result from mechanical hysteresis or from thermally-induced structural deformations of the instrument and are thus not accounted for by the gravitational flexure model. This method relies on measuring the centroid position of fiducial spots within each echellette image. The collimator is adjusted so that the positions of these spots match those in a reference image. These spots are produced by a small round hole in the slit mask located near one end of the slit. We discuss the design and calibration of this flexure compensation system and report on its performance on the telescope.

**Keywords:** active flexure compensation, Cassegrain spectrographs

## 1. INTRODUCTION

### 1.1. Motivation

As pointed out by Walker and D'Arrigo,<sup>1</sup> flexure within Cassegrain spectrographs results in image motion at the detector which reduces spectral and spatial resolution, degrades line profiles and radial velocities, and induces misalignment of flat fields. Such image motion requires observers to regularly obtain calibration arc spectra at representative telescope positions during observing, thereby wasting significant amounts of telescope time. While flexure might be reduced to acceptable levels using a carefully-tuned passive mechanical design,<sup>2</sup> they argue that reasonable constraints on mass, space, and cost may preclude such a solution, and that some form of active flexure compensation may prove more practical. Given the tight constraints of the Keck Telescope Cassegrain instrument envelope and mass budget, coupled with the goal of designing and building ESI quickly and inexpensively, provision for adding an open-loop, active flexure compensation system (FCS) was included in the initial ESI design.<sup>3</sup>

### 1.2. History

Experiments with the ISIS spectrograph at the Cassegrain focus of the 4.2-m William Herschel Telescope<sup>4</sup> have demonstrated both the potential benefits and limitations of using open-loop active compensation of spectrograph flexure. In those experiments, a fine-steering tip-tilt collimator was used as the active optical element. Using a look-up table providing first-order corrections derived from an all-sky flexure map, flexure-induced spectral drifts were reduced from 1.6 to 0.3 pixel (worst case) over a period of 4 hours of simulated telescope tracking. The reduction in image motion was limited not by the accuracy of the collimator adjustments but by several other factors, including

---

Further author information- (Send correspondence to R.K)

R.K.: Email: kibrick@ucolick.org; WWW: <http://www.ucolick.org/~kibrick>; Telephone: 831-459-2262; Fax: 408-429-5244;

J.M.: Email: miller@ucolick.org; Telephone: 831-459-2991; J.N.: Email: jnelson@ucolick.org; Telephone: 831-459-5132;

M.R.: Email: mvr@ucolick.org; Telephone: 831-459-2557; A.S.: Email: sheinis@ucolick.org; Telephone: 831-459-5881;

B.S.: Email: sutin@ociw.edu; Telephone: 626-304-0265

mechanical hysteresis, the accuracy of the flexure model, and changes in spectrograph settings. Long term stability of the flexure model was also a concern, with significant changes noted over a two month period.

A primary goal of the ESI mechanical design was to provide a rigid and optimally-constrained base for an active-collimator FCS. A related goal was to minimize structural hysteresis so that any residual flexure could be more reliably modeled. Accordingly, both the overall instrument structure,<sup>5</sup> the collimator support structure,<sup>6</sup> and most of the individual optical elements<sup>7</sup> were designed as determinate space-frame structures (see Fig. 1). The strut connections that mount the instrument to the rotator module are also a determinate structure and were designed to minimize stresses transferred from the module to the instrument. However, the design is not perfect due to manufacturing constraints. Consequently, a small amount of residual stress is transferred to the instrument (See Section 3.2). Although the preliminary design for the ESI FCS included both an active collimator and a piezoelectric actuator for adjusting the y-axis translation of the CCD,<sup>8</sup> a later sensitivity analysis determined that the collimator alone would be sufficient under the magnitudes of flexure predicted by the finite element analysis.

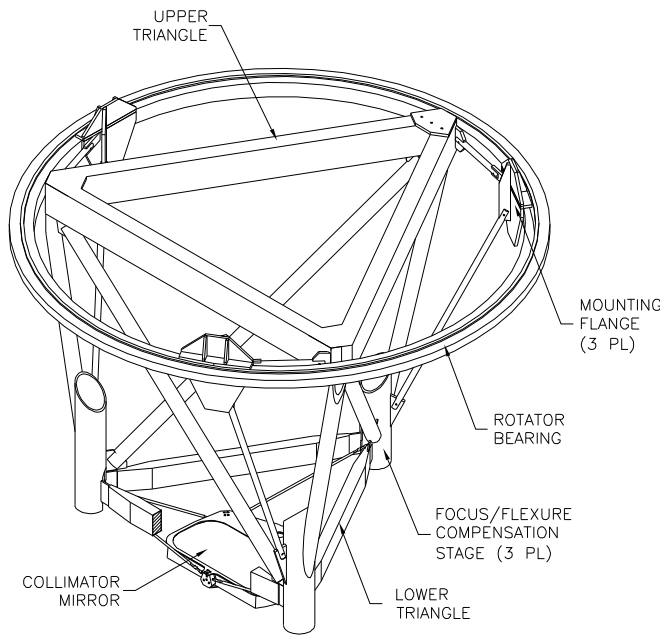


**Figure 1.** ESI structure.

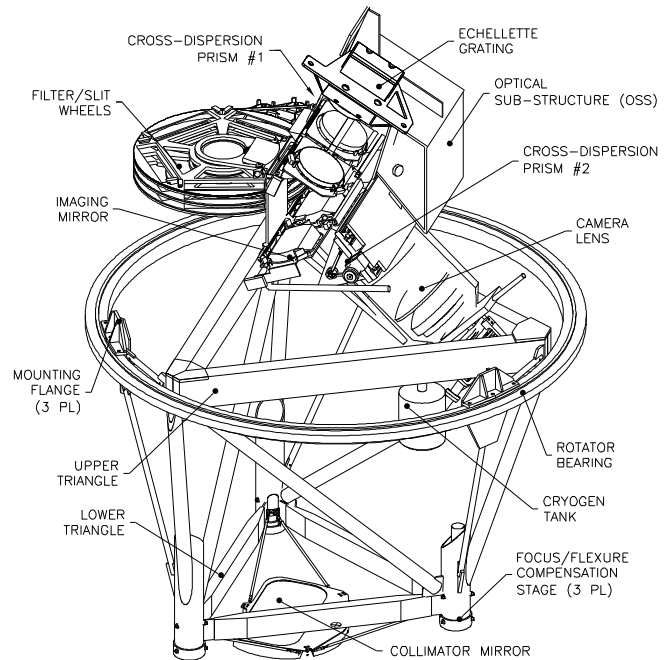


**Figure 2.** ESI instrument.

While it was decided early in the project to proceed with the low-level design and fabrication of the mechanical, optical, electronic, and software components of the active collimator mechanism, the decision to proceed with the higher-level FCS control software was deferred nearly to the end of the project. If the space-frame structures were able to passively reduce flexure to acceptable levels, then the FCS software would not be needed. Alternatively, if the hysteresis in the completed structure were too high, then an open-loop FCS system would not likely prove useful.

Initial flexure tests of the ESI instrument were conducted in the UCO/Lick Observatory instrument laboratory in Santa Cruz. The instrument was mounted in the Keck Cassegrain rotator module, which was in turn mounted to a structure that simulated the elevation motions of the telescope. Repeated sets of flexure measurements were obtained at elevation angles of 0, 30, 60, and 90 degrees and at 45 degree increments of rotator angle. Data were obtained for both clockwise and counter-clockwise rotations so as to measure hysteresis induced by the rotator mechanism. Early tests revealed significant image motion, due to movement of elements within the camera, inadequate nodal connections on the optical sub-structure (OSS), and non-optimal design of the struts which coupled the instrument to the rotator. Once these problems were corrected, both the residual flexure and hysteresis were determined to be sufficiently low to justify proceeding with implementation of the high-level FCS control software.

The FCS software was written while the instrument was being shipped to Hawaii, and received its first operational test during instrument commissioning at the Mauna Kea summit in September 1999. The flexure model was refined during subsequent engineering runs in October and November. The system became operational for science observing at the end of 1999 and is now in routine use.

### 1.3. Overview of collimator mechanism and optics

ESI has three operating modes: direct imaging, low-resolution, and echellette. Using a set of movable mirrors and prisms (each of which can be moved in or out of the light path), the collimated beam can either be directed to the camera for imaging, through a prism disperser, or to an echellette grating with prism cross-dispersion (see Fig. 2). Because the echellette mode captures the entire spectrum from 0.39 to 1.09 microns in a single exposure, the echellette grating operates at a fixed tilt. Thus, unlike ISIS, we are not concerned with changes in flexure that result from different settings of the grating tilt.

The ESI collimator mirror is located at the bottom of the Cassegrain instrument envelope. The collimator is approximately parabolic with its axis co-linear with the instrument and telescope axes. The three collimator actuators are designed as three independent cartridge assemblies that mount in the lower tubes of the main frame. These assemblies are moved in tandem to adjust collimator focus, while individual offsets are applied to adjust tip and tilt.

## 2. SYSTEM DESIGN

### 2.1. Hardware

Each collimator actuator assembly is composed of a THK High Precision ball screw (6-mm pitch) slide driven by a Galil servo-motor (4000 count/revolution encoder) through a 100:1 gearbox. Included in the assembly is a 1/10-micron Renishaw linear encoder used to implement a continuous dual-loop servo within a Galil Model DMC-1500 8-axis servo motor controller. The actuator servo system is capable of repeatable positioning to 0.04 arc second of collimator tilt (or 0.0012 arc second on the sky) over the entire 50-mm range of focus. The actuators can be operated manually using a hand paddle that connects directly to the Galil controller, or remotely from the computer control. The RS-232 serial interface on the Galil controller connects to a Lantronix ETS/8-P terminal server located within one of the insulated electronics enclosures mounted on the outside of the instrument structure. The terminal server connects to the control computer via a ThinNet Ethernet coaxial cable that runs through the instrument and telescope cable wraps.

### 2.2. Software

The high-level FCS software was implemented as a separate control task following the model successfully used for the Keck-I HIRES image rotator software.<sup>9</sup> The various components of the FCS software run on several different machines. Some of these components are part of the ESI control system, while others are part of the Keck Telescope Drive and Control System (DCS).<sup>10</sup>

#### 2.2.1. Low-level software: The ESI COLL keywords

Like all ESI mechanical stages, the collimator actuators are controlled using keywords<sup>11</sup> that are contained within the ESI keyword sharable library (`libesi_keyword.so`) and which are used in conjunction with the Keck Task Libraries (KTL). These keywords, which are similar in structure to FITS keywords, provide a simple and consistent applications programming interface (API) for interacting with the underlying hardware. For example, the current position of a stage can be obtained by reading the keyword corresponding to that stage; the stage can be commanded to a new position by writing a new value to that keyword. Callback routines can be mapped to specific keywords so that a callback is invoked whenever its associated keyword changes value. These same keywords are also used to document within FITS headers the position of each stage at the time a given image is taken. Observers generally do not use these keywords directly, since a graphical user interface (GUI), *dashboard* (see section 2.2.4), provides the primary method by which the observer operates the instrument. However, the ESI keywords can also be used directly from within various types of scripts (e.g., `csh`, `Tcl`) to perform automated sequences of commands for either diagnostic, calibration, or observational purposes.

Table 1 lists a subset of the ESI collimator actuator control keywords that were implemented to support the flexure compensation system. For ease of recognition, all of these keywords begin with the four letter prefix `COLL`. The `COLLFOC`, `COLLFOCR`, and `COLLFOCT` keywords are used in commanding simultaneous motions to all three actuators so as to piston the collimator and adjust focus. The `COLLFLXn` keywords are used by the FCS for adjusting collimator tip and tilt while the `COLLUSRn` keywords allow user-specified offsets to be added to those adjustments.

**Table 1.** ESI collimator keywords

Keyword	Function	Sense	Units or values
COLLMODE	Sets FCS operating mode	Read/Write	ON or OFF
COLLSTAT	FCS operational status	Read-only	String
COLLMSG	FCS error message	Read-only	String
COLLFOC	Collimator focus in microns	Read/Write	real microns
COLLFOCR	Collimator focus in counts	Read/Write	integer encoder counts
COLLFOCT	Collimator focus target	Read-only	integer encoder counts
COLLFLX1	FCS adjustment for actuator 1	Read/Write	integer encoder counts
COLLFLX2	FCS adjustment for actuator 2	Read/Write	integer encoder counts
COLLFLX3	FCS adjustment for actuator 3	Read/Write	integer encoder counts
COLLUSR1	User adjustment for actuator 1	Read/Write	integer encoder counts
COLLUSR2	User adjustment for actuator 2	Read/Write	integer encoder counts
COLLUSR3	User adjustment for actuator 3	Read/Write	integer encoder counts
COLLOFF1	Actuator 1 offset from commanded position	Read-Only	integer encoder counts
COLLOFF2	Actuator 2 offset from commanded position	Read-Only	integer encoder counts
COLLOFF3	Actuator 3 offset from commanded position	Read-Only	integer encoder counts

### 2.2.2. DCS keywords used by FCS

The Keck DCS has its own keyword sharable library (`libdcs_keyword.so`) which provides a similar style API for all of the various functions of the DCS. A subset of the DCS keywords are used to determine the current orientation of the telescope and the rotator module. Table 2 lists these DCS keywords, as well as several other DCS keywords used to indicate which instrument is currently receiving the light from the telescope.\* Like the ESI keywords, these DCS keywords are usually used via the command line interface or from within scripts only during tests or calibration procedures. They are primarily visible to observers via the FITS headers into which they are logged. The DCS provides several GUIs to allow the observing assistant (who operates the telescope) to control telescope and rotator positions.

**Table 2.** DCS keywords used by ESI FCS

Keyword	Function	Sense	Units or values
CURRINST	currently selected instrument	Read-Only	string
EL	telescope elevation angle	Read-Only	radians
FOCALSTN	currently selected focal station	Read/Write	enum
ROTDEST	rotator user specified destination	Read/Write	radians
ROTMODE	rotator tracking mode	Read-Write	†
ROTPDSTS	rotator physical-destination (2 Hz)	Read-Write	radians
ROTPOSN	rotator user achieved position	Read-Write	radians
ROTPPOSN	rotator physical achieved position	Read-Write	radians

### 2.2.3. The FCS task: *watch\_coll*

The ESI flexure compensation task is called *watch\_coll* and runs on the ESI supervisory computer. It communicates via keywords with the ESI dispatcher process, which runs on the same computer. The dispatcher in turn communicates with the Galil DMC-1500 motor controller. The dispatcher provides the read, write, and callback functions associated with each ESI motion control keyword, and provides the translation between keyword changes and low-level Galil motor controller operations. The *watch\_coll* task also communicates with several DCS VME-bus control crates (where the pointing task and ancillary telescope and dome control tasks run) by means of DCS keyword reads

\*Detailed descriptions of all DCS keywords are provided in Keck Software Document 46.

†Vertical angle, Position angle, or Physical angle.

that are transmitted over a separate 10 Mbit/sec public Ethernet link connecting the supervisory computer to the DCS crates.

At startup, the *watch\_coll* process uses the KTL operation *ktl\_read/continuous* to express interest in and establish callback routines for the DCS keywords that report the telescope elevation (EL) and instrument rotator physical angle (ROTPPOSN). Whenever the DCS broadcasts updated values for these keywords, the corresponding callback functions are invoked. If ESI is the currently selected instrument, then these callback invocations trigger recalculation of the flexure compensation model. That model computes the updated position of the collimator actuators appropriate for the current spectrograph mode (imaging, low-dispersion, or echellette) and the current position of the telescope and rotator. These updated positions are then transmitted to the ESI actuators by writing the corresponding COLLFLXn keywords. Although the flexure model is recalculated at 1 Hz. rate, corrections are not applied until the accumulated image motion reaches 0.1 pixel in magnitude so as to avoid unnecessary use of the collimator actuators. All three actuators are updated in parallel to minimize response time and mechanical stress on the collimator mechanism.

While the algorithm that transforms the correction from CCD pixel space to collimator actuator space is not purely focus neutral, in practice the contribution to focus change that results from operation of the FCS is below the detectable threshold. As a result, while the applied values of the COLLFLXn keywords will change periodically as the telescope tracks across the sky, the focus value reported by the COLLFOC keyword remains constant.

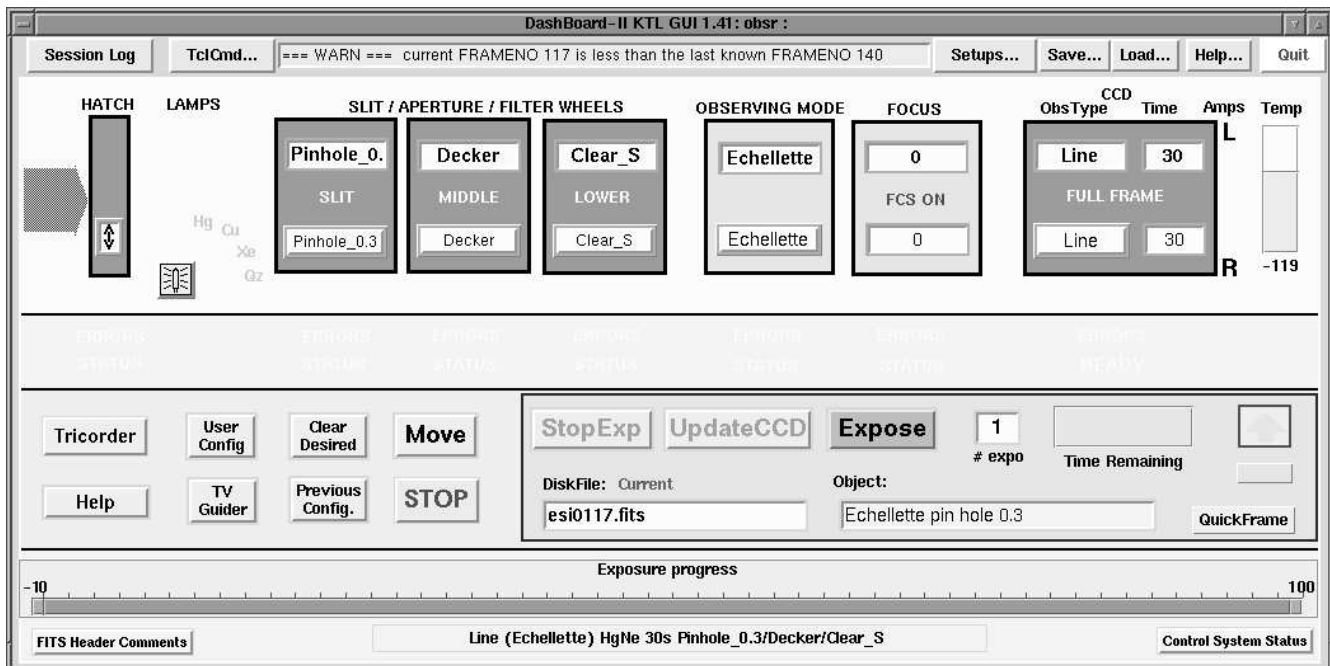
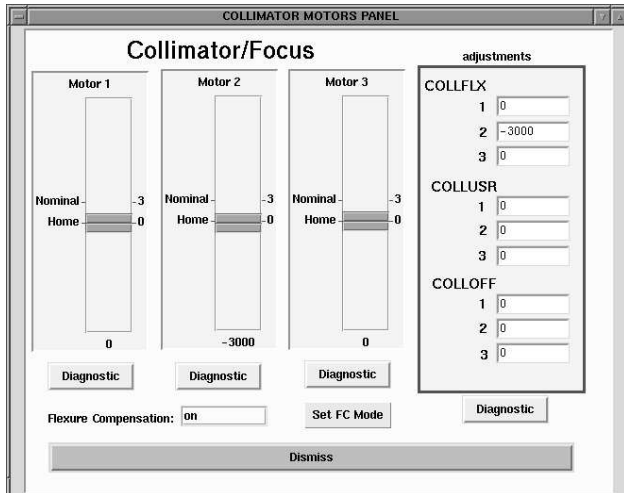


Figure 3. The ESI graphical user interface: **dashboard** interface.

#### 2.2.4. Modifications to the ESI graphical user interface: *dashboard*

The top-level window for the ESI graphical user interface (GUI), *dashboard*,<sup>12</sup> is shown in Fig. 3. This window provides a simplified view of the instrument and uses a graphical, linear representation of the light path to concisely display the state of all the major opto-mechanical elements of the instrument. This representation provides a clear and unambiguous display of the position of any optical elements that can be moved in or out of the light path, thus alerting observers to common errors in instrument setup. Cooperating copies of *dashboard* can be run at multiple sites, facilitating cooperative local/remote observing. The actual (top) and desired (bottom) settings for each component are shown within the icon for that component. For those components with a discrete number of settings, clicking on the desired setting brings up a pulldown menu of the available choices.



**Figure 4.** ESI collimator detail pop-up



**Figure 5.** Reference spots in echellette spectrum

To obtain additional detail on any component, the observer double-clicks on the icon for that component, causing a detail panel to pop-up. The detail panel for the collimators is shown in Fig. 4, and displays the current value of all the low-level collimator keywords. A slider graphic displays the relative positions of the three collimator actuators.

The FCS system does not require much interaction from the observer. From the ESI GUI, the observer can turn the FCS on or off, and review its current state via the collimator focus icon. In a future upgrade, a virtual strip chart displaying the most recent FCS actuator adjustments will be added.

### 2.2.5. Compensating for non-modeled errors

The ESI FCS system only compensates for those errors that can be modeled in terms of gravitational flexure. Non-modeled errors include those that result from changes in temperature across the instrument structure, from lost motion in optical stages and in the camera, and from small zero point shifts that are observed whenever the instrument is removed from and then re-inserted into the telescope. The cause of these zero point shifts is not yet understood and requires further analysis.

Two utility programs, *esitrim* and *esiadjust*, were implemented so that the observer can use the collimator to interactively steer the image on the detector. These are intended for use primarily during initial instrument setup at the start of the run. *Esitrim* is used to steer the image so as to compensate for the non-modeled errors, while *esiadjust* allows the observer to apply a specified offset so that specific spectral features can be steered away from CCD defects. *Esitrim* prompts the user to take a calibration image appropriate for the current spectrograph mode and to identify the positions of a standard set of features within that image. Those positions are then compared to the positions of corresponding features in a reference image in order to derive a set of offsets. Those offsets are then applied to the collimator actuators so that subsequent images taken in this mode will properly align with the reference image for that mode. Both the *esitrim* and *esiadjust* utilities apply their offsets via the COLLUSRn keywords, thus avoiding contention with the COLLFLXn keywords that are used by the *watch\_coll* process.

## 3. CALIBRATION

While the software effort required to implement the *watch\_coll* process was less than two man-weeks, the collection and reduction of the calibration data needed to compute the model coefficients involved significant effort and closed-dome telescope time. Since daytime telescope time is difficult to obtain on the Keck Telescopes due to ongoing telescope engineering and maintenance activities, most of the ESI FCS calibration was performed at night during inclement weather. In addition, it was performed remotely over Internet-2 from our Keck remote observing facility in Santa Cruz, California.<sup>13</sup>

### 3.1. Image motion versus collimator motion

Before spending any closed-dome telescope time on measuring ESI spectrograph flexure, we needed to demonstrate that we could reliably steer the image using the collimator. This was done when the instrument was not mounted in the telescope. Measurements of image motion versus collimator motion were obtained in all three instrument

modes to determine the relevant transformations and to verify that the system operated linearly. Image positions were measured by computing the centroid of a reference spot produced by a 0.3 arc-second pinhole in the slit mask located near one edge of the slit (see Fig. 5).

### 3.1.1. Motions of individual actuators

We first measured the image motions induced by individually moving each actuator by known amounts. Since there are three actuators but only two axes of the CCD (rows and columns), motion of a given actuator generally results in translation of the image in both axes of the CCD. These initial measurements verified the linearity of the system and determined the effective gain of each actuator relative to the two axes of the CCD.

However, due to anamorphic distortion from the two cross dispersing prisms in the two spectroscopic modes, the actual gain is not constant across the detector. In order to simplify the control algorithm, a specific image feature near the center of the detector was selected as the central reference for each instrument mode. The gains for each actuator were then determined for each instrument mode using their respective reference features. These same reference features were later used when determining the image motions induced by spectrograph flexure.

### 3.1.2. Motions of multiple actuators

In order to change the instrument focus on ESI it is desirable to move the collimator parallel to the instrument axis defined by the center of the Keck pupil and the center of the echellette slit (for example). To do this, ESI has three linear actuators attached to the collimator via six struts. If these actuators are parallel to the instrument axis and to each other, then moving all three actuators by the same amount will move the collimator along the instrument axis, refocusing the instrument without image motion.

If the actuators are not parallel to the instrument axis, but are parallel to each other, then an equal motion of the actuators will move the collimator along a different axis without tilt. In this case, the collimator will translate relative to the image, producing refocus with a small (probably negligible) image motion. However, if the actuators are not parallel to each other, then the collimator will tilt as it focuses, resulting in image motion when focusing.

When the instrument was first assembled in Santa Cruz, the three actuators were aligned parallel to each other using a granite block. Each actuator was swept with an indicator until it was perpendicular to the block. When the instrument was re-assembled after shipment to the Mauna Kea summit, we were unable to align the collimator actuators because we did not have the ability to point the instrument at zenith outside the telescope nor did we have a granite block available at the summit. Measurements of ESI image motion obtained at the summit after moving all three actuators simultaneously by the same amount demonstrated that the actuators were no longer parallel to each other.

Although it was not originally intended that it perform such compensation, the *watch\_coll* task was quickly modified to compensate for image motion induced by changing the collimator focus. The effect is quite linear and is easily modeled. Separate calibrations were performed for each instrument mode using their respective central reference features.

## 3.2. Image motion versus spectrograph orientation

Measurements of image motion induced by spectrograph flexure were obtained with the instrument and rotator module installed in the Keck II Telescope. Line lamp calibration spectra were obtained in the two spectroscopic modes and images of the echellette slit were obtained in imaging mode. These spectra and images were obtained over a standard grid of telescope elevation angles and rotator angles. The telescope was stepped in elevation between 0, 30, 60, and 90 degrees. At each of these four elevations, calibration data were obtained at 17 different rotator positions, sampling two full revolutions (one clockwise, one counterclockwise) in increments of 45 degrees of rotation. By rotating in both directions, we were able to check for rotation-induced hysteresis, which was found to be significant. Unfortunately, there was not adequate engineering time available to traverse elevation in both directions.

All flexure measurements were made using the same central reference features for each mode as were used to calibrate both the actuator gains and the actuator axes misalignments. The results of the flexure measurements obtained during the October 1999 engineering run are shown for all three instrument modes as Figs. 7-9. A repeat measurement of flexure in the echellette mode was obtained during the November run and is shown in Fig. 6. Note that in low-dispersion mode, the dispersion direction is parallel to the rows (or X axis) of the CCD, while in echellette mode, due to the grating cross-dispersion, the dispersion direction is parallel to the columns (or Y axis).

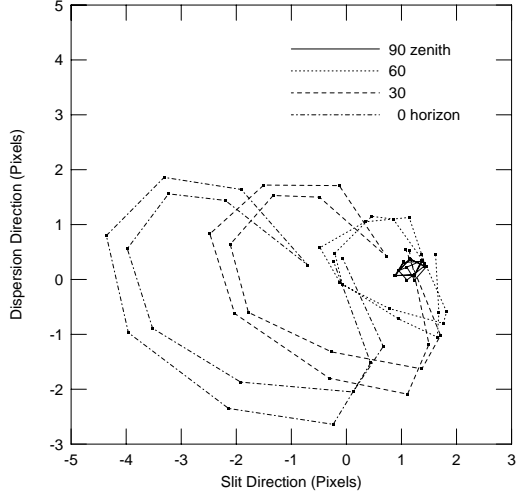


**Figure 6.** Flexure map: echellette mode (November)

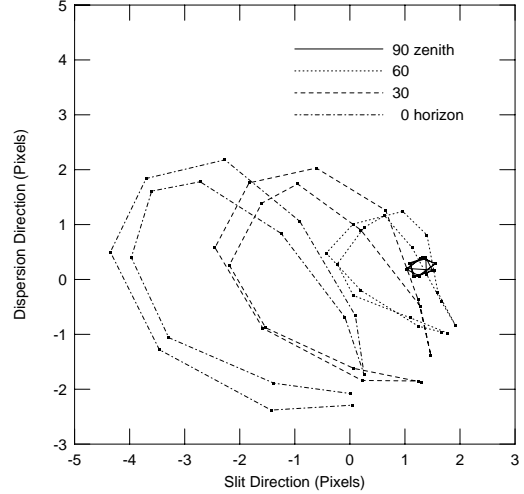


**Figure 7.** Flexure map: echellette mode (October)

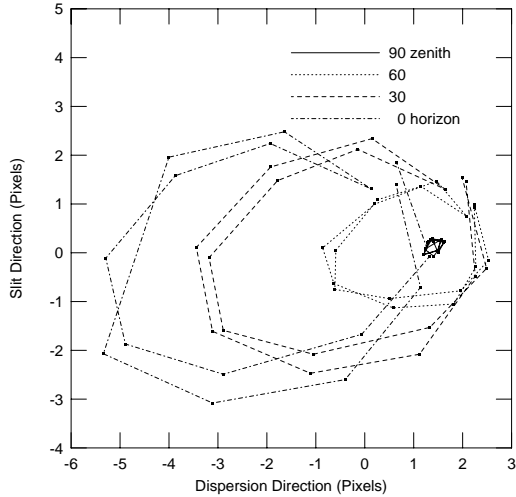


**Figure 8.** Flexure map: low-resolution mode (Oct.)

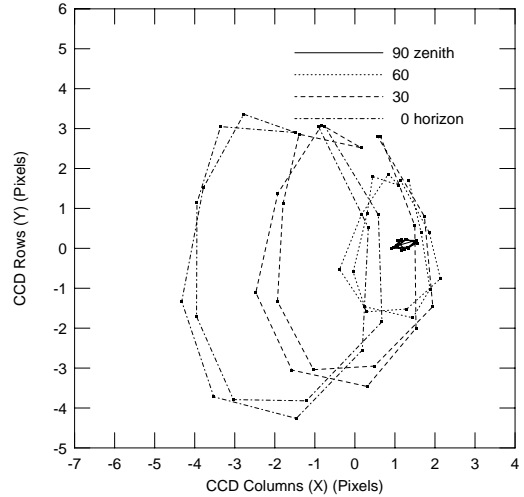


**Figure 9.** Flexure map: imaging mode (Oct.)

These plots show an unexpected result. If the telescope is pointing at the zenith, the orientation of the instrument relative to gravity remains constant when the instrument is rotated. There should be no gravitationally-induced flexure, and the zenith data points should appear coincident on the plot. However, these points (shown connected with solid lines) are not coincident but rather show a small but repeatable image motion that correlates with instrument rotation. There is out-of-roundness or runout between the instrument and the rotator module. The determinate structure that attaches ESI to the rotator module isolates most of the bearing stresses from the instrument. A small amount of residual stress contributes to the observed hysteresis and zenith motion. Image motions induced by such stresses are neither modeled nor corrected by our model of gravitationally-induced flexure.

#### 4. MODELING

Given the space-frame structures used for ESI, a linear elasticity model of gravitational flexure was used for fitting the image motion versus spectrograph position data. This differs from the approach described by Munari, in which a set of orthogonal polynomials was used.<sup>14</sup> The equations for this gravitational flexure model are as follows:

$$X(\phi, \theta) = a_0 + a_1 \cos \phi \cos \theta + a_2 \cos \phi \sin \theta + a_3 \sin \phi \quad (1)$$

$$Y(\phi, \theta) = b_0 + b_1 \cos \phi \cos \theta + b_2 \cos \phi \sin \theta + b_3 \sin \phi \quad (2)$$

where  $X$  is the predicted position of the reference spot in the  $X$  (or column) axis of the CCD,  $Y$  the predicted position in the  $Y$  (row) axis,  $\phi$  the telescope elevation angle,  $\theta$  the rotator physical angle, and the  $a_i$  and  $b_i$  the coefficients obtained from a least square fit of the data to the model. Each instrument mode is fit separately.



The gravitational flexure model provided a relatively good fit to the observed data for all three modes. The worst-case residuals (vector magnitude of X and Y residuals) in each mode were: imaging mode, 0.63 pixels; low resolution mode, 0.66 pixels; echellette mode, 0.64 pixels. The corresponding RMS residual errors were: imaging mode, 0.29 pixels; low resolution mode, 0.25 pixels; echellette mode, 0.25 pixels. These residuals are not unreasonable given the non-modeled image motions observed at zenith plus the several tenths of a pixel hysteresis observed at all positions. Since one pixel corresponds to 0.153 arc-seconds on the sky, worst-case residuals were about 0.1 arc-seconds and RMS residuals were about 0.04 arc-seconds.

## 5. OPERATIONAL PERFORMANCE

Since the ESI FCS system has only been used to date for a small number of nights, only limited data on its operational performance is currently available.<sup>15</sup>

### 5.1. Calibration run

To validate the gravitational flexure model and the overall operation of the FCS, the sequence of images described in section 3.2 was repeated for each mode, except this time the FCS system was turned on. The results of these measurements are shown for all three instrument modes as Figs. 11-13. These represent worst case errors over the entire sky. For a typical exposure, residual errors would be a few tenths of a pixel, or about 0.04 arc-seconds on the sky. By comparing these to the corresponding measurements obtained with the FCS turned off (see Figs. 7-9), it is clear that the FCS has significantly reduced flexure-induced image motion in all three modes.

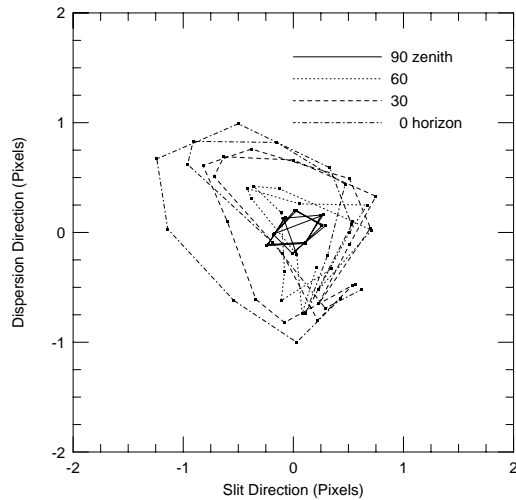


Figure 10. Residual errors Echellette mode (Nov.)

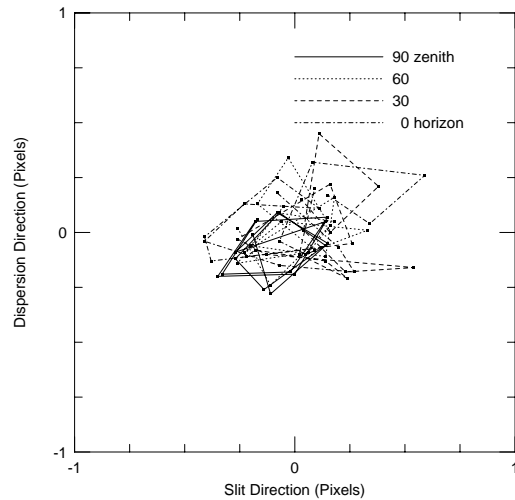


Figure 11. Residual errors: Echellette mode (Oct.)

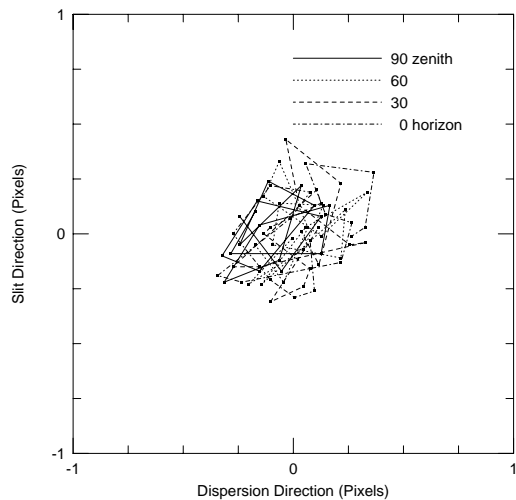


Figure 12. Residual errors: Low-res. mode (Nov.)

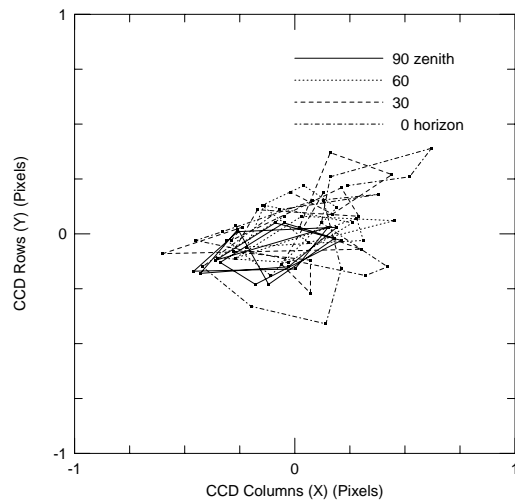


Figure 13. Residual errors: Imaging mode (Nov.)

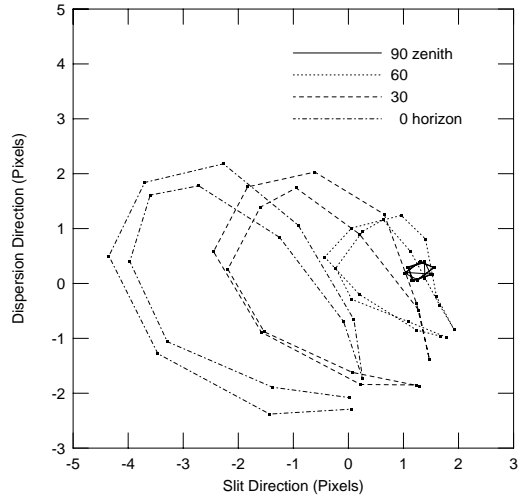


Figure 14. Motion of central spot, FCS off

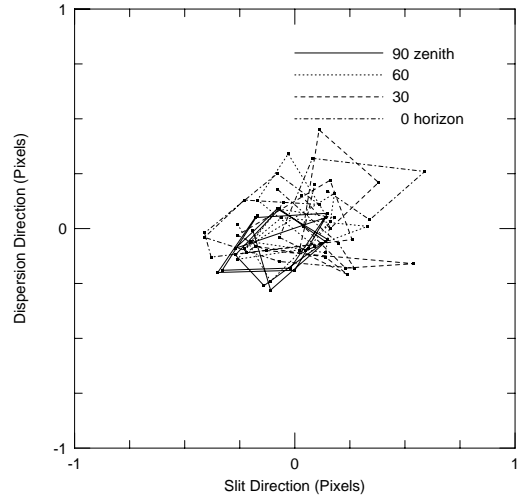


Figure 15. Motion of central spot, FCS on

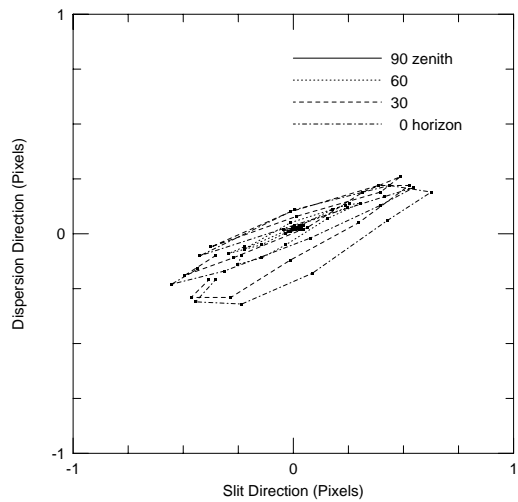


Figure 16. Vertical difference, FCS off

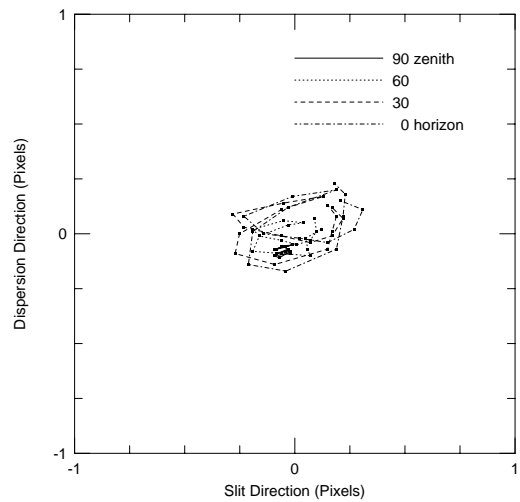


Figure 17. Vertical difference, FCS on

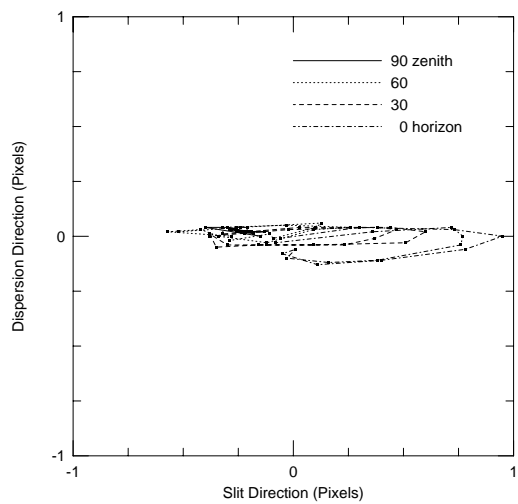


Figure 18. Horizontal difference, FCS off

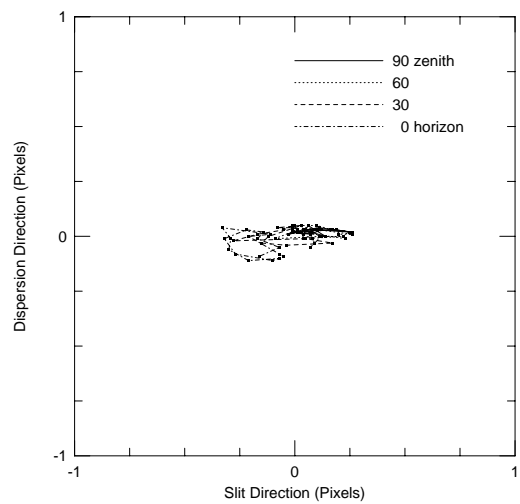


Figure 19. Horizontal difference, FCS on

A repeat measurement of FCS performance in the echellette mode was obtained during the November run and is shown in Fig. 10. Comparing Figs. 10 and 11 reveals that the performance of the FCS system has degraded significantly over the period of one month. Note that the instrument was removed from the telescope after the October run and various mechanical adjustments were made to internal baffles.

The measurements depicted in Figs. 10-13 only demonstrate how well the single, central reference feature was stabilized for each instrument mode. To confirm whether stabilizing this feature was sufficient to stabilize the image across the entire CCD, a more extensive analysis of the echellette mode FCS calibration data was performed. That analysis found no significant field rotations, and only slight scale changes on the order of a few tenths of a pixel across the length and width of the detector. Thus, the entire image was stabilized. With the FCS system turned on, both image motion and the scale change in the slit direction were significantly reduced, while scale change in the dispersion direction was unchanged.

Figs. 14-19 show the flexure performance of the spectrograph in echellette mode with and without FCS for the October run. Figures 14 and 15 are for a spot centrally located at pixel (1400,2022), which was the spot used to generate the FCS model. Figures 16 and 17 are the difference in position between two spots at pixel (1242,3888) and pixel (1550,625), which are near the opposite ends of the 9<sup>th</sup> order. A large width in the vertical direction would imply a large change in echellette dispersion, but is not seen. Figures 18 and 19 are the difference in position between two spots at pixel (1986,2004) and pixel (600,1998), which are near the center of the 6<sup>th</sup> and 14<sup>th</sup> orders. A large width in the horizontal direction would imply a large relative motion along the echellette slit, as well as a large change in the low-resolution mode dispersion.

## 5.2. Operational concerns

In order for the FCS to correctly compensate for ESI instrumental flexure, the FCS relies on the DCS to provide the current telescope elevation angle and Cassegrain rotator angle. Due to daily telescope maintenance activities, the DCS is often uninitialized during the daytime and thus it is unable to provide this information to the FCS. Under existing operational policy, DCS initialization typically does not occur until 5 p.m HST. As a result, any ESI line lamp comparison spectra or flat fields taken while the DCS is uninitialized will not be correctly compensated for ESI flexure and will thus not register correctly with spectra taken after DCS initialization is complete. This constraint prevents efficient use of the instrument during the daytime. Since the flexure compensation model requires only a coarse measurement of the telescope and rotator angles, future instruments planning an FCS may want to consider including their own independent means of measuring these angles via some type of tilt-measuring device.

## 6. CONCLUSION

The ESI FCS has been successfully commissioned on Keck II. Image motion due to flexure has been reduced by a factor of ten to a few tenths of a pixel for a typical exposure. Image motion induced by refocusing the spectrograph has been effectively eliminated. The long term stability of the calibrations is unknown and should be periodically rechecked, especially since this can now be done automatically and during the daytime if telescope maintenance activities don't conflict. A compensation-off flexure map for echellette mode was obtained during both the October and November ESI engineering runs (See Figs. 7 and 6). The differences between these two maps is significant, and results in different model coefficients (See Table 3). Had coefficients derived from the November flexure map been used for the November FCS-on measurements, the compensation would likely have improved.

Mechanical hysteresis is significant and comparable to flexure residuals, especially when the telescope is operating at lower elevations. Fig. 20 plots the absolute value of the difference between the coordinates of the echellette mode central reference feature as observed on pairs of observations obtained at the same elevation and rotator angles but arrived at from opposite directions of rotator motion. It is clear that hysteresis increases significantly with increasing elevation angle. The mechanical sources for this hysteresis should be investigated, and if possible, reduced.

## ACKNOWLEDGMENTS

We thank Teresa Chelminiak, Bob Goodrich, Gary Puniwai, and Ron Quick of Keck Observatory for their assistance in collecting the closed-dome flexure tests. Goodrich also contributed significantly to the reduction and analysis of the ESI flexure data. Jim Burrous and Dean Tucker developed the low-level motor control software for all of the ESI stages, including the collimator actuators. De Clarke developed the ESI GUI, *dashboard*. We also acknowledge Elizabeth Chock, Al Conrad, and Julia Simmons for their assistance in commissioning the overall software for ESI.

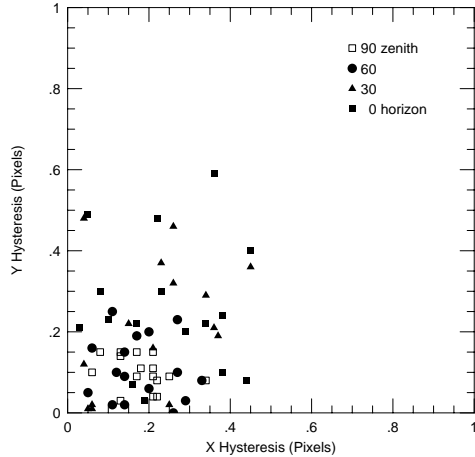


Figure 20. Hysteresis of paired points

Term	October 1999	November 1999
$a_0$	1397.24	1382.72
$a_1$	$1.498 \pm 0.049$	$1.577 \pm 0.054$
$a_2$	$1.544 \pm 0.051$	$1.632 \pm 0.051$
$a_3$	$3.278 \pm 0.064$	$3.074 \pm 0.068$
$\sigma$	0.20 pixels	0.21 pixels
$b_0$	2023.98	2024.08
$b_1$	$-2.088 \pm 0.037$	$-2.024 \pm 0.037$
$b_2$	$0.561 \pm 0.039$	$0.583 \pm 0.035$
$b_3$	$0.316 \pm 0.049$	$0.503 \pm 0.047$
$\sigma$	0.15 pixels	0.15 pixels

Table 3. Echellette mode model terms and statistics

## REFERENCES

1. D. D. Walker and P. D'Arrigo, "On the stability of Cassegrain spectrographs," *Mon. Not. R. Astron. Soc.* **281**, pp. 673–678, 1996.
2. H. Nicklas *et al.*, "Image motion and flexure compensation for the FORS spectrograph," in *Optical Astronomical Instrumentation*, S. D'Odorico, ed., *Proc. SPIE* **3355**, pp. 93–104, 1998.
3. H. W. Epps and J. S. Miller, "Echellette spectrograph and imager (ESI) for Keck Observatory," in *Optical Astronomical Instrumentation*, S. D'Odorico, ed., *Proc. SPIE* **3355**, pp. 48–58, 1998.
4. P. D'Arrigo, F. Diego, and D. D. Walker, "Active compensation of flexure on the WHT ISIS spectrograph," *Mon. Not. R. Astron. Soc.* **281**, pp. 679–686, 1996.
5. B. C. Bigelow and J. E. Nelson, "Determinate space-frame structure for the Keck II echellette spectrograph and imager (ESI)," in *Optical Astronomical Instrumentation*, S. D'Odorico, ed., *Proc. SPIE* **3355**, pp. 164–174, 1998.
6. M. Radovan, B. C. Bigelow, J. E. Nelson, and A. Sheinis, "Design of a Collimator support to provide Flexure Control on Cassegrain Spectrographs," in *Optical Astronomical Instrumentation*, S. D'Odorico, ed., *Proc. SPIE* **3355**, pp. 155–163, 1998.
7. A. Sheinis *et al.*, "Kinematic translation mechanism for moderate-sized optics," in *Optomechanical Engineering and Vibration Control*, E. A. Derby *et al.*, ed., *Proc. SPIE* **3786**, pp. 350–361, 1999.
8. B. M. Sutin, "ESI: a new spectrograph for the Keck II telescope," in *Optical Telescopes of Today and Tomorrow: Following in the Direction of Tycho Brahe*, A. Ardeberg, ed., *Proc. SPIE* **2871**, pp. 1116–1125, 1996.
9. R. Kibrick, A. Conrad, J. Gathright, and D. Tucker, "User Interface and Control Software for the HIRES Image Rotator on Keck-1," in *Telescope Control Systems II*, H. Lewis, ed., *Proc. SPIE* **3112**, pp. 187–198, 1997.
10. W. Lupton, H. Lewis, and A. Honey, "W. M. Keck Telescope control system," in *Advanced Technology Optical Telescopes V*, L. M. Stepp, ed., *Proc. SPIE* **2199**, pp. 638–644, 1994.
11. A. R. Conrad and W. F. Lupton, "The Keck Keyword Layer," in *Astronomical Data Analysis and Software Systems II*, R. J. Hanisch, R. J. V. Brissenden, and J. Barnes, eds., *ASP Conference Series* **52**, pp. 203–207, 1993.
12. D. Clarke, "Dashboard: a knowledge-based real-time control panel," in *Proceedings of the 5th Annual Tcl/Tk Workshop*, pp. 9–18, 1997.
13. R. Kibrick, S. Allen, and A. Conrad, "Remote observing with the Keck Telescopes from the U.S. mainland," in *Advanced Global Communications Technologies for Astronomy*, R. Kibrick and A. Wallander, eds., *Proc. SPIE* **4011**, 2000.
14. U. Munari and M. G. Lattanzi, "Flexures of Conventional Cassegrain-Fed Spectrographs," *Publ. Astron. Soc. of the Pacific* **104**(672), pp. 121–126, February 1992.
15. A. Sheinis, J. Miller, and M. Bolte, "Performance characteristics of the new Keck Observatory Echelle spectrograph and imager," in *Optical and IR Telescope Instrumentation and Detectors*, M. Iye and A. F. Moorwood, eds., *Proc. SPIE* **4008**, 2000.